





Geophysical Research Letters®



RESEARCH LETTER

10.1029/2023GL105180

Arctic Warming and Eurasian Cooling: Weakening and Reemergence

Xinping Xu¹ , Shengping He^{2,3,4} , Botao Zhou¹ , Huijun Wang^{1,3,5}, and Bo Sun^{1,3,5} 

Key Points:

- The significant Arctic mid-tropospheric warming and Eurasian cooling observed in winters before the 2010s has weakened in the past decade
- The combined effects of Arctic Oscillation and Ural blocking dominate the intensity of Arctic mid-tropospheric warming and Eurasian cooling
- Strong Eurasian cooling may reemerge before the 2050s if the atmospheric internal variability overwhelms the effects of greenhouse gases

Supporting Information:

Supporting Information may be found in the online version of this article.

Correspondence to:

S. He,
Shengping.He@uib.no

Citation:

Xu, X., He, S., Zhou, B., Wang, H., & Sun, B. (2023). Arctic warming and Eurasian cooling: Weakening and reemergence. *Geophysical Research Letters*, 50, e2023GL105180. <https://doi.org/10.1029/2023GL105180>

Received 11 JUL 2023
Accepted 26 OCT 2023

¹Collaborative Innovation Center on Forecast and Evaluation of Meteorological Disasters/Key Laboratory of Meteorological Disaster, Ministry of Education, Nanjing University of Information Science & Technology, Nanjing, China, ²Geophysical Institute, University of Bergen and Bjerknes Centre for Climate Research, Bergen, Norway, ³Nansen-Zhu International Research Centre, Institute of Atmospheric Physics, Chinese Academy of Sciences, Beijing, China, ⁴Nansen Environmental and Remote Sensing Center, Bergen, Norway, ⁵Southern Marine Science and Engineering Guangdong Laboratory (Zhuhai), Zhuhai, China

Abstract The observed Eurasian winter surface cooling from the 1990s to the early 2010s, which is contrary to global warming, has been extensively studied. Previous studies revealed that the surface cooling trend has significantly weakened in the past decade. Based on large-ensemble simulations, this study reveals that the weakening of Eurasian surface cooling is primarily driven by the atmospheric internal variability, which coincides with the weakening of Arctic mid-tropospheric warming and Eurasian mid-tropospheric cooling. Negative Arctic Oscillation (−AO) and Ural blocking (UB) in combination dominate the intensity of Arctic mid-tropospheric warming and Eurasian mid-tropospheric cooling. In the future, there is a possibility that the severe Eurasian cooling trend with comparable magnitude to that during 1990–2013 may reemerge accompanied with Arctic mid-tropospheric warming, in response to the decadal strengthening of −AO and UB. This may occur before the 2050s, when the atmospheric internal variability is able to overwhelm the effects of greenhouse gases.

Plain Language Summary The significant Eurasian surface cooling trend observed in winters from the 1990s to the early 2010s has significantly weakened in the past decade. It coincides with the weakened trends of Arctic mid-tropospheric warming and Eurasian mid-tropospheric cooling. In a warming world, we suggest that the weakening of Arctic mid-tropospheric warming and Eurasian mid-tropospheric and surface cooling are primarily caused by the atmospheric internal variability. The weakened trends of negative Arctic Oscillation (−AO) and Ural blocking (UB) in recent years contribute to the weakened trends of Arctic mid-tropospheric warming and Eurasian cooling. There is a possibility that the atmospheric internal variability may overwhelm the effects of increasing greenhouse gases (GHG) sometime before the 2050s, though the increasing GHG dominate the long-term increase of air temperature. Then, the strong negative trend of AO and intensified UB may lead to the reemergence of the severe Eurasian cooling trend before the 2050s.

1. Introduction

The Arctic surface has been warming dramatically in recent four decades, three to four times faster than the greenhouse gases (GHG)-induced global warming (Rantanen et al., 2022). The surface-amplified Arctic warming can extend throughout the troposphere in winter (i.e., December–February) (Cohen et al., 2020; X. Xu et al., 2019), characterized as a deep Arctic warming (He et al., 2020). Arctic warming has been revealed to be associated with the observed severe winter cooling trend (Cohen et al., 2014) and cold extremes (Liu et al., 2012) over Eurasia from the early 1990s to the 2010s. However, the diversity of Eurasian temperature responses to Arctic forcing among different numerical simulations makes the Arctic-midlatitude teleconnection more controversial (Francis, 2017; Outten et al., 2023; Screen et al., 2018).

Recent studies (He et al., 2020; X. Xu et al., 2021) highlighted the importance of the vertical extension of Arctic warming on resolving the differences of Arctic-midlatitude linkage in climate models. Numerical simulations verified that the vertical extent of Arctic warming can induce remarkable midlatitude circulation changes and colder-than-normal Eurasia, while shallow Arctic warming can not (He et al., 2020; Labe et al., 2020). Midlatitude circulation responses depend on the depth of winter Arctic warming in idealized experiments (Sellevold et al., 2016). There is also evidence to link Eurasian winter cooling trend to the Arctic troposphere (Ye et al., 2018).

© 2023. The Authors.

This is an open access article under the terms of the [Creative Commons Attribution-NonCommercial-NoDerivs License](https://creativecommons.org/licenses/by/4.0/), which permits use and distribution in any medium, provided the original work is properly cited, the use is non-commercial and no modifications or adaptations are made.

Despite the critical role of deep Arctic warming in favoring the Arctic-Eurasia linkage, the mechanism of deep Arctic warming remains insufficient (Cohen et al., 2020). Arctic sea ice reduction has been revealed as the major cause of Arctic surface warming, due to ice-albedo feedback and more heat release from the ocean to the atmosphere during cold seasons (Cohen et al., 2014; Screen & Simmonds, 2010). A recent study hypothesized the effect of Arctic sea ice loss in driving Arctic mid-to-upper tropospheric warming by stratosphere-troposphere coupling (M. Xu et al., 2023). Remote factors such as poleward heat and moisture transport are important contributors to the winter Arctic warming aloft (Screen et al., 2012; Suo et al., 2022). Low-latitude sea surface temperature (SST) forcing can drive large-scale atmospheric circulation changes at high latitudes that induce Arctic tropospheric warming (Ding et al., 2014; Perlwitz et al., 2015) and that inhibit Arctic summer surface warming and sea-ice melting on interannual timescale (Hu et al., 2016). In addition, the atmospheric internal variability is supposed to explain a significant proportion of Arctic tropospheric warming (Graversen et al., 2008). Cohen et al. (2020) revealed that most coupled and uncoupled climate models show a lack of Arctic tropospheric warming signal. Only part of individual ensemble members can reproduce the vertical distribution of Arctic tropospheric warming, suggestive of the effect of the atmospheric internal variability (Ogawa et al., 2018; X. Xu et al., 2019). In summary, most of the existing research agreed with the important role of atmospheric variability, which involves the unpredictable internally generated variability and the atmospheric circulation changes caused by boundary and radiative forcings (Deser et al., 2016).

Interestingly, we note that the significant Arctic mid-tropospheric warming observed in winters before the early 2010s has been decreasing, despite the ongoing surface warming (Figures 1a–1d). The decreasing Arctic mid-tropospheric warming is in contrast to the rising anthropogenic warming. Meanwhile, the remarkable Eurasian surface cooling trend has substantially weakened in recent years (Blackport & Screen, 2020; Outten et al., 2023). Why does the Arctic mid-tropospheric warming weaken in a warming world? The atmospheric internal variability is hypothesized to be the cause. Previous studies have revealed the contributions of large-scale atmospheric circulation patterns, such as Arctic Oscillation (AO) and atmospheric blocking, to the Arctic-Eurasian surface temperature trend (Mori et al., 2014; Ye & Messori, 2020). This paper will focus on the effects of specific atmospheric patterns on modulating the intensity of Arctic mid-tropospheric warming and Eurasian mid-tropospheric cooling.

2. Data and Methods

Monthly atmospheric data including surface air temperature (SAT), temperature and geopotential height at 500 hPa (T500 and Z500), and zonal wind at 300 hPa (U300) are employed from: (a) the fifth generation European Center for Medium-Range Weather Forecasts reanalysis (ERA5) for 1979–2021 (Hersbach et al., 2020); (b) the 40-member ensemble of historical simulations for 1979–2005 and future projections for 2006–2100 of the Community Earth System Model (CESM) Large Ensemble (CESM-LENS) (Kay et al., 2015). Each ensemble member in the CESM-LENS is subject to identical radiative forcing but with a small random noise difference (order of 10^{-14} K) to initial atmospheric conditions. The data are linearly detrended before correlation, regression, and empirical orthogonal function (EOF) analyses. The linear trends are computed using linear regression analysis. The standard Student's *t* test is employed for statistical significance of correlation and regression analyses. The degree of freedom is $n - 2$ (n is the number of samples). Winter of 2020 refers to December in 2020 and January and February in 2021.

Barents-Kara Seas (BKS; 70°N–80°N, 30°E–70°E; blue frame in Figure 1a) (He et al., 2020) and northeastern Canada-Greenland (NCG; 55°N–85°N, 20°W–80°W; green frame in Figure 1a) (Ding et al., 2014) are two strong warming centers over the Arctic. Two Arctic mid-tropospheric temperature indices (ATI_500_BKS and ATI_500_NCG) are defined as area-averaged T500 over the BKS and the NCG, respectively. The Eurasian mid-tropospheric temperature index (ETI_500) and surface temperature index (ETI_2m) are respectively defined as area-averaged T500 and SAT over Central Eurasia (CE; 40°N–60°N, 60°E–120°E; red frame in Figure 1a) (Mori et al., 2014). The UB index (UBI) is defined as area-averaged Z500 over 45°N–80°N and 10°W–80°E (Peings, 2019). The monthly AO index (AOI) is obtained from the Climate Prediction Center of NOAA (https://www.cpc.ncep.noaa.gov/products/precip/CWlink/daily_ao_index/ao.shtml). The Northern Hemisphere annual mode (NAM) index (NAMI) is defined as the difference of area-averaged U300 between 35°N–40°N, 0°E–360°E and 55°N–60°N, 0°E–360°E (blue and red frames in Figure S2a in Supporting Information S1) based on L'Heureux and Thompson (2006). The NAMI which is highly related to the AOI with a correlation of 0.88

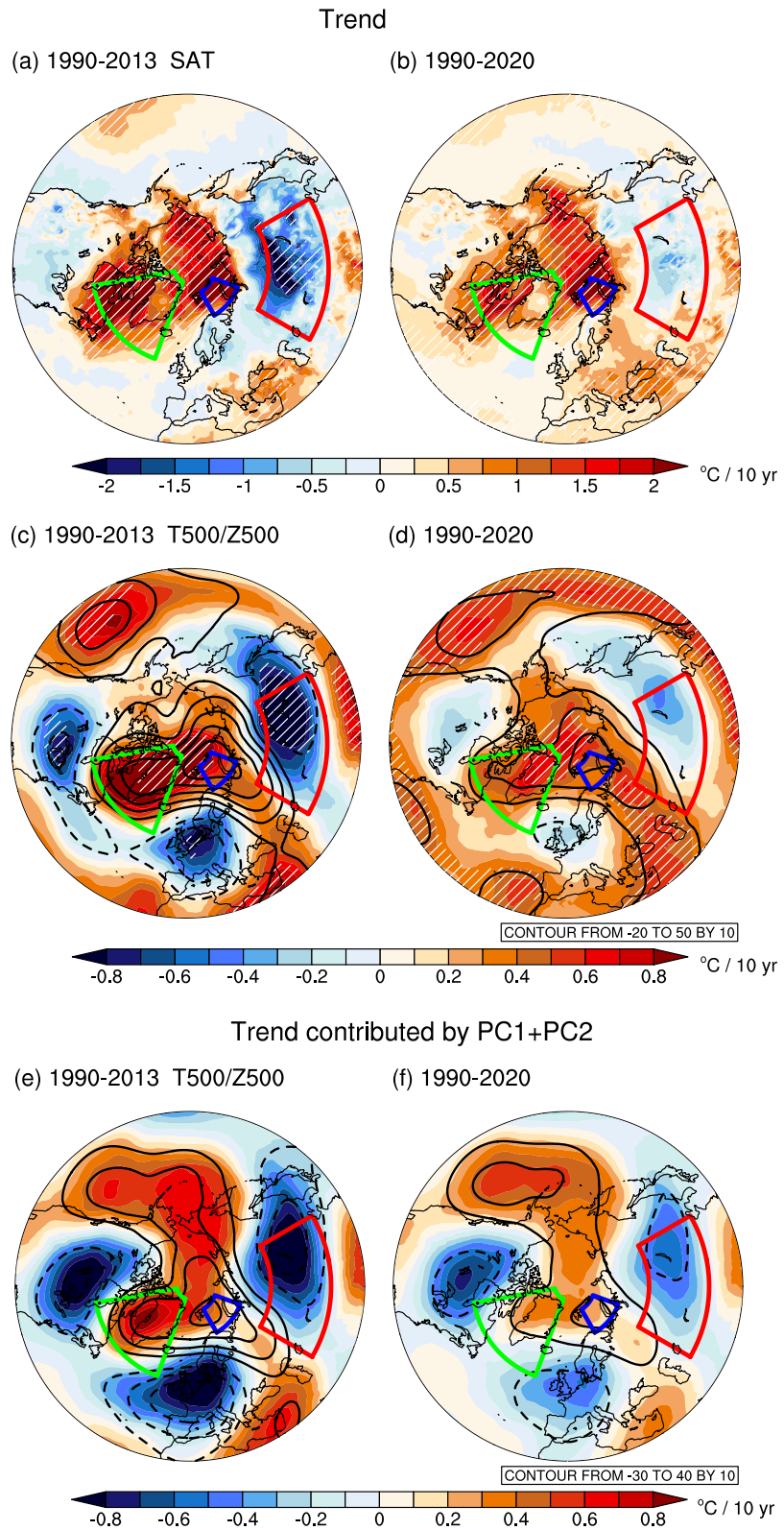


Figure 1. (a–b) Linear trends of surface air temperature (SAT) ($^{\circ}\text{C decade}^{-1}$) during winters of (a) 1990–2013 and (b) 1990–2020 from European Center for Medium-Range Weather Forecasts reanalysis (ERA5). (c–d) Same as (a–b), but for T500 ($^{\circ}\text{C decade}^{-1}$; shading) and Z500 (m decade^{-1} ; contours). Regions with temperature trends statistically significant at the 95% confidence level are marked with slash. (e–f) Same as (c–d), but for linear trends of T500 and Z500 estimated by the sum of PC1 and PC2.

(Figure S2b in Supporting Information S1), is used to represent AO in CESM-LENS simulations. The results are robust using both AOI and NAMI from the reanalysis data. All indices are normalized. For winters of 2023–2050 in the CESM-LENS, the 10-year period with the concurrence of strong negative trend of AO and positive trend of UB is identified when both the negative NAMI (–NAMI) and positive UBI have a trend exceeding 1.5 standard deviation/decade. When different periods overlap in one ensemble member, the 10-year period with the strongest trends of –NAMI and UBI will be selected.

3. Results

3.1. Observations: Weakened Trends of Arctic Mid-Tropospheric Warming and Eurasian Mid-Tropospheric Cooling in Recent Years

Figures 1a–1d compare the trends of winter temperature and atmospheric circulation north of 30°N between 1990–2013 and 1990–2020. The Eurasian surface cooling trend has significantly weakened in the past decade (Figures 1a vs. 1b). But no significant weakening of surface warming is detected over the BKS (Figures 1a vs. 1b). Interestingly, Arctic mid-tropospheric warming has substantially weakened in recent years, coinciding with the weakened trends of Eurasian surface and mid-tropospheric cooling (Figures 1a–1d; shading). Large-scale atmospheric circulation trends have correspondingly reduced, including the weakening of the trends toward the anticyclone/cyclone over the Arctic/midlatitudes (Figures 1c and 1d; contours). The Arctic anticyclonic circulation contributes to tropospheric warming through adiabatic heating (Ding et al., 2014) and poleward moisture transport (X. Xu et al., 2021). The mid-latitude trough causes northerly cold advection and thus cold conditions over Eurasia (Mori et al., 2014). Changes in the trends of large-scale atmospheric circulation are generally observed in strength but not spatial pattern, indicating that some specific atmospheric circulation patterns may modulate the intensity of Arctic mid-tropospheric warming and Eurasian mid-tropospheric cooling.

The dominant modes of mid-tropospheric atmospheric circulation are extracted by performing EOF analysis to Z500 anomalies north of 30°N during winters of 1979–2020. The leading EOF mode is primarily characterized as AO, and the second mode features a pronounced wave train-like structure from the North Atlantic to Eurasia and a Pacific–North America pattern (PNA) (Figures S1a and S1b in Supporting Information S1). The corresponding principal components (PC1 and PC2) show strong positive trends during 1990–2013 (0.69/decade and 0.69/decade) but relatively weak trends during 1990–2020 (0.27/decade and 0.52/decade) (Figures S1e–S1f in Supporting Information S1). The time series of PC1 highly correlates with the AOI ($r: -0.98$), both of which are associated with T500 over the NCG ($r: 0.81/-0.79$) and CE ($r: -0.55/0.54$) (Figures S1c and S1e in Supporting Information S1). EOF2 correlates significantly with UB ($r: 0.37$) which is critical for BKS warm anomalies ($r: 0.62$) and Eurasian cold anomalies ($r: -0.72$) (Figures S1d and S1f in Supporting Information S1). Reduction in the upward trends of PC1/negative AOI and PC2/UBI from 1990–2013 to 1990–2020 coincides with the weakening of Arctic mid-tropospheric warming and Eurasian mid-tropospheric cooling (Figures S1e–S1g in Supporting Information S1). The PNA pattern does not correlate significantly with Arctic mid-tropospheric temperature and its intensity does not exhibit obvious trend during 1990–2013 or 1990–2020 (Figure not shown).

The potential contribution of atmospheric circulation patterns to Arctic mid-tropospheric warming and Eurasian mid-tropospheric cooling is further examined (Figures 1e and 1f). The linear trend of Z500 contributed by PC1 and PC2 in combination (i.e., PC1 + PC2) is calculated by multiplying the PC1/PC2 trend with the regression coefficients of Z500 (i.e., contours in Figures S1c and S1d in Supporting Information S1) and then linearly combining the estimated trend of Z500 related to PC1 and that related to PC2 (Ye & Messori, 2020). The linear trend of T500 contributed by PC1 + PC2 is calculated in the same way. As shown by Figure 1e, PC1 + PC2 can capture the main characteristics of the observed trends of mid-tropospheric circulation and temperature north of 30°N during 1990–2013. The spatial correlation coefficient (SCC) between the observed and estimated Z500/T500 trends reaches up to 0.92/0.78. The trend toward higher/lower geopotential heights contributes to Arctic/Eurasian mid-tropospheric warming/cooling (Figure 1e). Ye and Messori (2020) found that leading atmospheric modes dominate the trend of Eurasian surface cooling but cannot explain Arctic surface warming. Different from surface warming, Arctic mid-tropospheric warming can be largely captured by PC1 + PC2 (Figure 1e). For 1990–2020, the estimated weakened trends of mid-tropospheric circulation and temperature contributed by PC1 + PC2 (Figure 1f) also resemble those in observations, with a SCC of 0.82/0.55 in the Z500/T500 field. Therefore, the two main atmospheric modes may dominate the trend of mid-tropospheric temperature north of 30°N. In other words, the decreasing trends of negative AO and positive UB may account for the weakening of Arctic mid-tropospheric warming and Eurasian mid-tropospheric cooling in the past decade.

3.2. CESM-LENS Historical Simulations: Role of Atmospheric Circulation Patterns

Outputs from large ensemble CESM-LENS simulations (Kay et al., 2015) are further employed to investigate the role of specific atmospheric circulation patterns. The simulated winter Z500 and T500 trends vary widely across individual members (Figures S3 and S4 in Supporting Information S1). This is the result of internal variability as each ensemble member only differs in initial atmospheric conditions with a small random noise. Uniform warming in the ensemble-mean is indicative of the role of external forcing (e.g., GHG). Figure 2a exhibits the spatial correlation coefficients between the simulated and observed T500 trends and the spatial correlations between the simulated and observed Z500 trends for 1990–2013. When one ensemble member shows large (small) pattern correlation with observations in the Z500 trend field, it will also show large (small) pattern correlation with observations in the T500 trend field (Figure 2a). The linear relationship in both periods (Figures 2a and 2b) implies the important role of atmospheric dynamics in impacting the mid-tropospheric temperature.

To verify the atmospheric contributions to the weakened trend of the mid-tropospheric temperature in recent years, two groups of ensemble members that best capture the observed Z500 trend associated with PC1 + PC2 for 1990–2013 and for 1990–2020 are selected respectively. The degree of similarity is determined by the SCC and root mean square difference (RMSD) between the simulated Z500 trend (i.e., contours in Figures S3 and S4 in Supporting Information S1) and the observed Z500 trend related to PC1 + PC2 (i.e., contours in Figures S1c and S1d in Supporting Information S1). Taking the period of 1990–2013 for example, we first select 20% of the 40 ensemble members that show the highest SCC; then, we selected 50% of the “20% high SCC ensembles” that have the lowest RMSD. The “10% high SCC-low RMSD ensembles,” hereafter referred to as Ensemble-A, best captures the observed trends of two main atmospheric modes north of 30°N during 1990–2013. For 1990–2020, we select another “10% high SCC-low RMSD ensembles” using the same method as above, hereafter referred to as Ensemble-B.

As shown in Figures 2c and 2d, the simulated Z500/T500 trend bears great resemblance to the observed Z500/T500 trend associated with PC1 + PC2 for 1990–2013 (SCC: 0.87/0.67) and for 1990–2020 (SCC: 0.83/0.62). The trends toward an anticyclonic circulation over the Arctic and a cyclonic circulation over Eurasia in Ensemble-A bring the strong response of Arctic mid-tropospheric warming and Eurasian mid-tropospheric cooling (Figure 2c). Tropospheric temperature changes are considered as an adiabatic response to upper-level atmospheric circulation changes (Ding et al., 2014). The simulated strong negative trend of AO favors intense mid-tropospheric warming over the NCG (Figures 2c and 3a). The simulated BKS warming at 500 hPa is primarily driven by the intensified UB (Figures 2c and 3c). The time series of simulated $-NAMI/UBI$ is highly consistent with that of ATI_500_NCG/ATI_500_BKS with a correlation coefficient of 0.75/0.85, close to the correlation coefficient in ERA5 (0.73/0.72). Moreover, the surface and mid-tropospheric cooling trends over Eurasia in response to atmospheric forcing (Figures 2c, 2e, and 3e) have similar pattern and comparable magnitude to those in observations (Figures 1a and 1c and Figure S1g in Supporting Information S1). In Ensemble-B, the weakened trends of atmospheric circulation patterns contribute to the weakened trends of Arctic mid-tropospheric warming and Eurasian cooling (Figures 2d and 2f). The negative trend in NAMI and positive trend in UBI are reduced by $\sim 0.4/\text{decade}$ and $\sim 0.2/\text{decade}$ respectively, leading to comparable reduction in the trends of ATI_500_NCG , ATI_500_BKS , and ETI_2m (Figure 3). The observed changes in the intensity of Arctic mid-tropospheric warming and Eurasian cooling are well reproduced by a small proportion of ensemble members that capture changes in the intensity of specific atmospheric circulation patterns, suggestive of the critical role of the atmospheric internal variability. It is noteworthy that the results are not sensitive to the selection criteria of ensemble members (Figure S5 in Supporting Information S1) or different sets of model simulations (e.g., CMIP6) (Figure not shown).

3.3. Strong Eurasian Cooling May Reemerge in the Future

Some studies have attributed the observed Eurasian surface cooling trend from the 1990s to the early 2010s to the atmospheric internal variability (Ogawa et al., 2018). The weakening of the cooling trend after the early 2010s is hypothesized related to other climate variability than Arctic surface warming (Blackport & Screen, 2020). In this study, results based on CESM-LENS historical simulations suggest that the atmospheric variability is an important driving factor for the weakening of Arctic mid-tropospheric warming and Eurasian cooling in the past decade. On this basis, will strong Eurasian cooling trend reemerge in the future if large-scale atmospheric circulation patterns exhibit similar trends like those during 1990–2013?

It cannot be denied that the increasing GHG concentrations play a dominant role in driving the long-term increase of air temperature (IPCC, 2021). The simulated winter temperature over Eurasia will increase by ~ 5 to $\sim 10^\circ\text{C}$

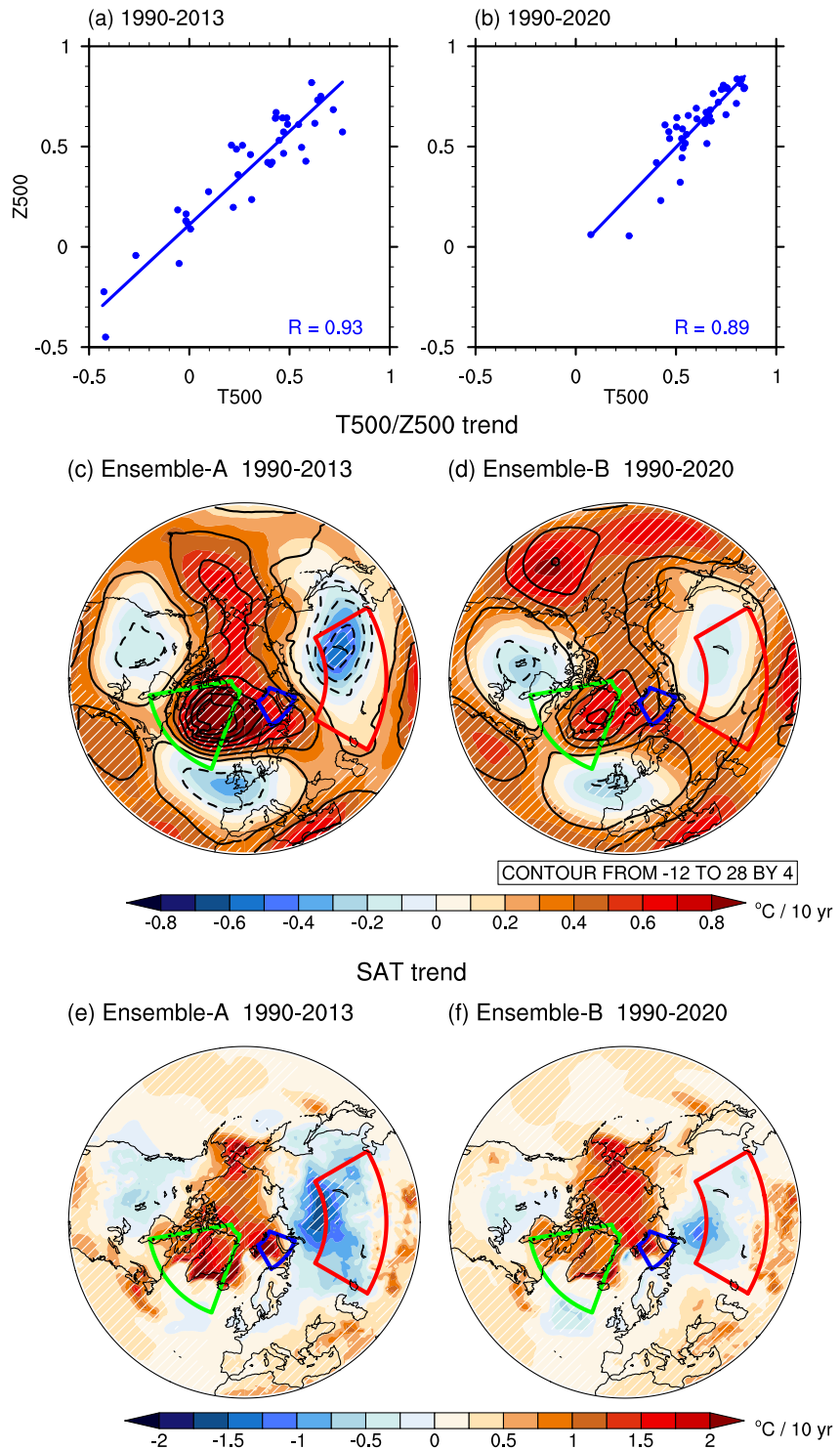


Figure 2. (a–b) Spatial correlation correlations between the observed and simulated T500/Z500 trends north of 30°N from 40 ensemble members of the Community Earth System Model–Large Ensemble (CESM–LENS) during winters of (a) 1990–2013 and (b) 1990–2020. (c–d) Linear trends of T500 (°C decade⁻¹; shading) and Z500 (m decade⁻¹; contours) during winters of (c) 1990–2013 from Ensemble-A and (d) 1990–2020 from Ensemble-B of the CESM–LENS. (e–f) Same as (c–d), but for surface air temperature (SAT) (°C decade⁻¹). Regions with temperature trends statistically significant at the 95% confidence level are marked with slash.

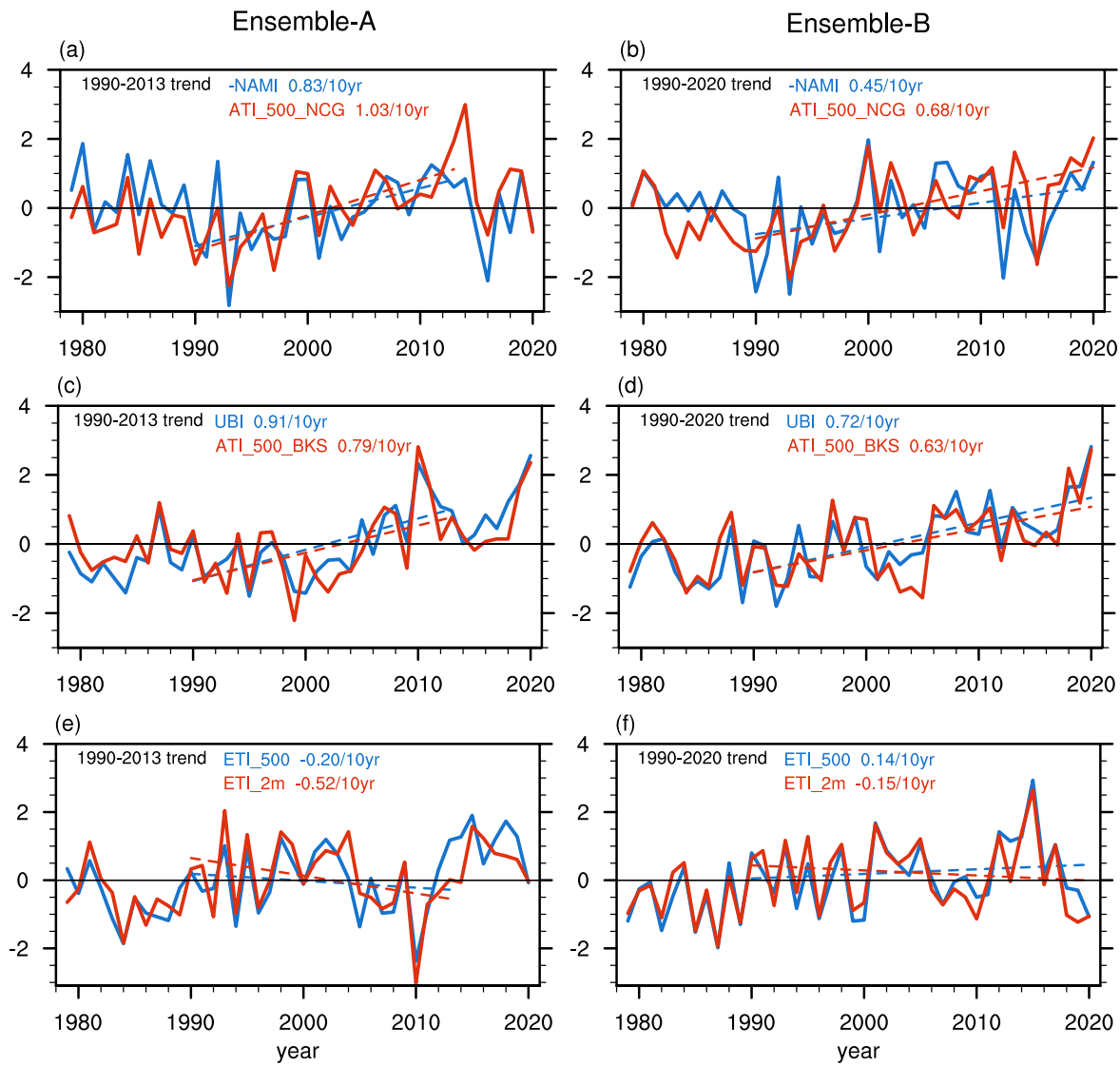


Figure 3. (a–b) Time series of negative Northern Hemisphere annual mode index (NAMI) (blue lines) and ATI_500_NCG (red lines) during winters of 1979–2020 from (a) Ensemble-A and (b) Ensemble-B of the Community Earth System Model–Large Ensemble (CESM–LENS). The dashed lines denote linear trends during (a) 1990–2013 and (b) 1990–2020. (c–d) And (e–f) same as (a–b), but for (c–d) UBI (blue lines) and ATI_500_BKS (red lines), and (e–f) ETI_500 (blue lines) and ETI_2m (red lines).

at the end of the century in CESM–LENS future projections (Figure S6 in Supporting Information S1). In addition, the internally generated Eurasian temperature will exhibit decadal fluctuations that can superimpose on the long-term warming trend, leading to alternative emergence of warmer and colder conditions before the 2050s (Figure S6 in Supporting Information S1). This suggests a possibility that the atmospheric internal variability may overwhelm the effects of GHG sometime in the future and may lead to the reemergence of Eurasian cooling trend.

We have identified the 10-year period with the concurrence of strong negative trend of AO and positive trend of UB during 2023–2050 from 10 individual members of the CESM–LENS (Figure S7 in Supporting Information S1). In total, 11 cases are selected. In response to the combined effects of AO and UB, the projected temperature field will exhibit strong Arctic mid-tropospheric warming trend and strong Eurasian mid-tropospheric cooling trend (Figure 4a). At surface, the projected cooling trend of Eurasia has a similar pattern and comparable magnitude to the observed one during 1990–2013 (Figures 4b vs. 1a). Stronger decadal changes of AO and UB may give rise to greater response of Eurasian cooling (Figure 4c), suggestive of the chance of extreme surface cooling in the

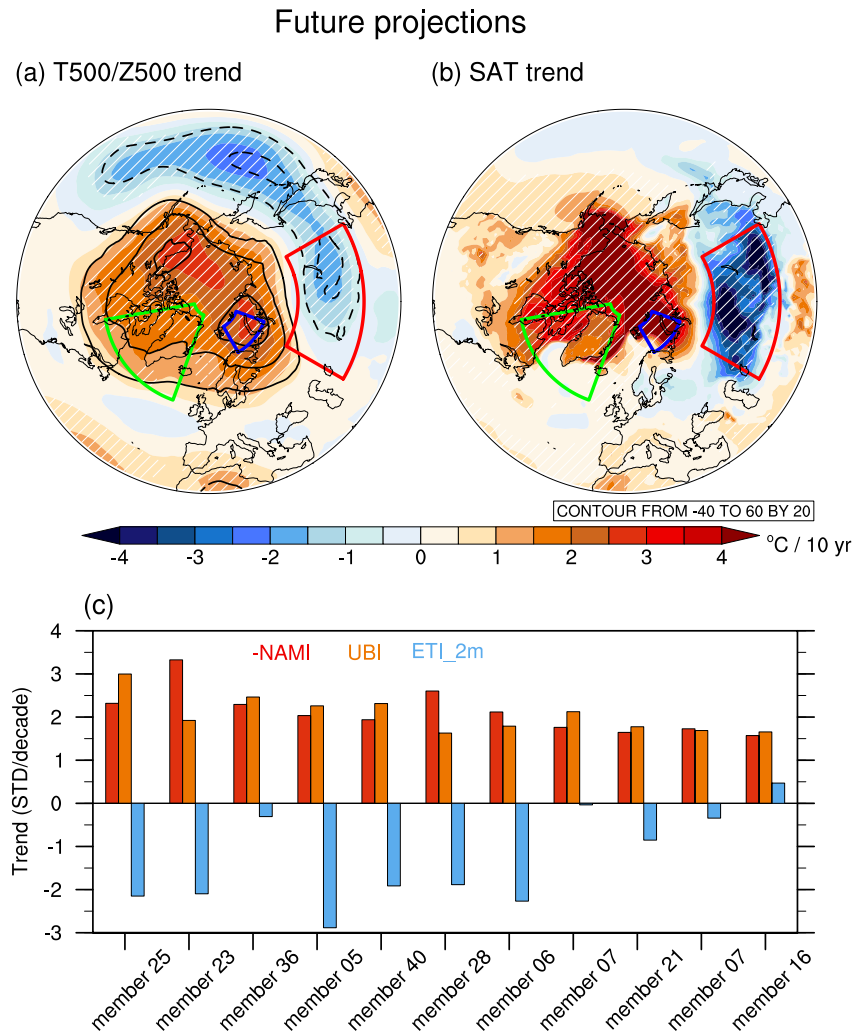


Figure 4. (a) Composited mean linear trends of T500 ($^{\circ}\text{C decade}^{-1}$; shading) and Z500 (m decade^{-1} ; contours) for 11 cases with the strongest 10-year upward trends of negative Northern Hemisphere annual mode index (NAMI) and positive UBI, during winters of 2023–2050 from 10 ensemble members of the Community Earth System Model–Large Ensemble (CESM–LENS). (b) Same as (a), but for surface air temperature (SAT) ($^{\circ}\text{C decade}^{-1}$). Regions with temperature trends statistically significant at the 95% confidence level are marked with slash. (c) Linear trends of the negative NAMI, UBI and ETI_2m for the 11 cases.

future. Moreover, the reemergence of the severe cooling trend may coincide with extremely colder-than-normal winters (Figure S7 in Supporting Information S1). The results of future projections suggest a possibility of the reemergence of Arctic mid-tropospheric warming and Eurasian cooling in the future. Note that Arctic surface warming is highly coupled with sea ice decline (Screen & Simmonds, 2010) under increasing GHG. The projected strong Arctic surface warming (Figure 4b) will be dominated by the increasing GHG rather than the atmospheric internal variability.

4. Conclusions and Discussions

The remarkable Eurasian surface cooling trend observed in winters from the 1990s to the early 2010s has significantly weakened in the past decade, concurrent with the weakening of Arctic mid-tropospheric warming and Eurasian mid-tropospheric cooling. This study investigates the combined effects of two leading atmospheric circulation modes (i.e., EOF1 and EOF2 of Z500 north of 30°N) on modulating the intensity of Arctic mid-tropospheric warming and Eurasian mid-tropospheric cooling. PC1 and PC2 in combination can largely capture the trends of Arctic mid-tropospheric warming and Eurasian mid-tropospheric cooling during 1990–2013

as well as the weakening trends during 1990–2020. More specifically, the EOF1 mode is highly related to negative AO and the EOF2 mode correlates significantly with UB in the Arctic-Eurasian sector. The combined effects of AO and UB are hypothesized to dominate the intensity of Arctic mid-tropospheric warming and Eurasian mid-tropospheric cooling.

Results from CESM-LENS simulations support the role of the atmospheric internal variability in modulating the intensity of Arctic mid-tropospheric warming and Eurasian mid-tropospheric cooling. A small proportion of ensemble members that best capture the intensity of specific atmospheric patterns (i.e., AO and UB) during 1990–2013 and during 1990–2020 can well reproduce the increasing of Arctic mid-tropospheric warming and Eurasian mid-tropospheric cooling during 1990–2013 and their weakening trends during 1990–2020. The projected Eurasian winter temperature will exhibit decadal fluctuations, superimposing on the long-term warming driven by increasing GHG concentrations. There is a possibility that Arctic mid-tropospheric warming and Eurasian cooling may reemerge sometime before the 2050s, when the atmospheric internal variability may overwhelm the effects of GHG. In response to the combination of strong negative trend of AO and intensified UB before 2050, intense Eurasian surface cooling trend may occur with comparable magnitude to that during 1990–2013.

Mori et al. (2014) attributed the severe Eurasian winters during 1979–2013 to the combination of the negative phase of AO and positive phase of the warm Arctic-cold Eurasia pattern, the latter of which is related to the blocking anticyclone over the Urals. Extending the results of Mori et al. (2014), we primarily focus on the combined effects of atmospheric circulation patterns (i.e., AO and UB) on modulating the intensity of Arctic mid-tropospheric warming and Eurasian mid-tropospheric cooling. In terms of the relative effect of AO and UB, it is estimated that the negative trend of AO is more important than intensified UB in causing the pattern of Arctic warming and Eurasian cooling (Figure S8 in Supporting Information S1). This is reasonable because the EOF1 mode of Eurasian winter temperature is highly associated with AO (Mori et al., 2014). Moreover, the combined effects of AO and UB can force even stronger Eurasian cooling trend (Figure 4b) than the Eurasian cooling caused by individual AO or UB (Figure S8 in Supporting Information S1). This further emphasizes the importance of the combined effects of AO and UB.

The predominantly internally generated AO and UB can be modulated by different boundary forcing such as Arctic sea ice (Kim et al., 2014), Eurasian snow cover (Henderson et al., 2018; X. Xu et al., 2018) and remote SST forcing (Chen et al., 2023; Jeong et al., 2022). A recent study revealed that the Indian ocean warming plays a role in driving the positive trend of AO through momentum flux convergence by the stationary waves and troposphere-stratosphere coupling over the North Pacific (Jeong et al., 2022). In this sense, the warming trend of the Indian Ocean may force the tendency toward a positive AO in recent years. The influences of other forcing factors on the weakened trends of AO and UB in recent years need further investigation.

Data Availability Statement

Data used in this study are available:

- (1) ERA5: <https://cds.climate.copernicus.eu/cdsapp#!/search?type=dataset&text=ERA5>.
- (2) CESM-LENS: <https://www.cesm.ucar.edu/experiments/cesm1.1/LE/>.
- (3) AO index: https://www.cpc.ncep.noaa.gov/products/precip/CWlink/daily_ao_index/ao.shtml.

References

- Blackport, R., & Screen, J. A. (2020). Weakened evidence for mid-latitude impacts of Arctic warming. *Nature Climate Change*, *10*(12), 1064–1066. <https://doi.org/10.1038/s41558-020-00954-y>
- Chen, X., Hu, C., & Tao, L. (2023). Unexpected cooling Eurasia during February of global-warming slowdown: Roles of North Atlantic and Arctic Oceans. *Atmospheric Research*, *294*, 106969. <https://doi.org/10.1016/j.atmosres.2023.106969>
- Cohen, J., Screen, J. A., Furtado, J. C., Barlow, M., Whittleston, D., Coumou, D., et al. (2014). Recent Arctic amplification and extreme mid-latitude weather. *Nature Geoscience*, *7*(9), 627–637. <https://doi.org/10.1038/ngeo2234>
- Cohen, J., Zhang, X., Francis, J., Jung, T., Kwok, R., Overland, J., et al. (2020). Divergent consensus on Arctic amplification influence on midlatitude severe winter weather. *Nature Climate Change*, *10*(1), 20–29. <https://doi.org/10.1038/s41558-019-0662-y>
- Deser, C., Terray, L., & Phillips, A. S. (2016). Forced and internal components of winter air temperature trends over North America during the past 50 years: Mechanisms and implications*. *Journal of Climate*, *29*(6), 2237–2258. <https://doi.org/10.1175/jcli-d-15-0304.1>
- Ding, Q., Wallace, J. M., Battisti, D. S., Steig, E. J., Gallant, A. J. E., Kim, H.-J., & Geng, L. (2014). Tropical forcing of the recent rapid Arctic warming in northeastern Canada and Greenland. *Nature*, *509*(7499), 209–212. <https://doi.org/10.1038/nature13260>

Acknowledgments

This research was supported by the Guangdong Major Project of Basic and Applied Basic Research (Grant 2020B0301030004), the Research Council of Norway projects MAPARC (Grant 328943) and BASIC (Grant 325440), the National Natural Science Foundation of China (Grant 42075030), and the Natural Science Foundation of the Jiangsu Higher Education Institutions of China (Grant 23KJB170013).

- Francis, J. A. (2017). Why are Arctic linkages to extreme weather still up in the air? *Bulletin of the American Meteorological Society*, 98(12), 2551–2557. <https://doi.org/10.1175/bams-d-17-0006.1>
- Graversen, R. G., Mauritsen, T., Tjernström, M., Källén, E., & Svensson, G. (2008). Vertical structure of recent Arctic warming. *Nature*, 451(7174), 53–56. <https://doi.org/10.1038/nature06502>
- He, S., Xu, X., Furevik, T., & Gao, Y. (2020). Eurasian cooling linked to the vertical distribution of Arctic warming. *Geophysical Research Letters*, 47(10), e2020GL087212. <https://doi.org/10.1029/2020gl087212>
- Henderson, G. R., Peings, Y., Furtado, J. C., & Kushner, P. J. (2018). Snow-atmosphere coupling in the Northern Hemisphere. *Nature Climate Change*, 8(11), 954–963. <https://doi.org/10.1038/s41558-018-0295-6>
- Hersbach, H., Bell, B., Berrisford, P., Hirahara, S., Horányi, A., Muñoz-Sabater, J., et al. (2020). The ERA5 global reanalysis [Dataset]. Quarterly Journal of the Royal Meteorological Society, 146(730), 1999–2049. <https://doi.org/10.1002/qj.3803>
- Hu, C., Yang, S., Wu, Q., Li, Z., Chen, J., Deng, K., et al. (2016). Shifting El Niño inhibits summer Arctic warming and Arctic Sea ice melting over the Canada Basin. *Nature Communications*, 7(1), 11721. <https://doi.org/10.1038/ncomms11721>
- IPCC 2021 Climate Change. (2021). *The physical science basis. Contribution of Working Group I to the sixth assessment report of the Intergovernmental Panel on Climate Change*. Cambridge University Press.
- Jeong, Y.-C., Yeh, S.-W., Lim, Y.-K., Santoso, A., & Wang, G. (2022). Indian Ocean warming as key driver of long-term positive trend of Arctic Oscillation. *npj Climate and Atmospheric Science*, 5(1), 56. <https://doi.org/10.1038/s41612-022-00279-x>
- Kay, J. E., Deser, C., Phillips, A., Mai, A., Hannay, C., Strand, G., et al. (2015). The Community Earth System Model (CESM) large ensemble project: A community resource for studying climate change in the presence of internal climate variability [Dataset]. Bulletin of the American Meteorological Society, 96(8), 1333–1349. <https://doi.org/10.1175/BAMS-D-13-00255.1>
- Kim, B. M., Son, S. W., Min, S. K., Jeong, J. H., Kim, S. J., Zhang, X., et al. (2014). Weakening of the stratospheric polar vortex by Arctic sea-ice loss. *Nature Communications*, 5(1), 4646. <https://doi.org/10.1038/ncomms5646>
- Labe, Z., Peings, Y., & Magnusdottir, G. (2020). Warm Arctic, cold Siberia pattern: Role of full Arctic amplification versus sea ice loss alone. *Geophysical Research Letters*, 47(17), e2020GL088583. <https://doi.org/10.1029/2020gl088583>
- L'Heureux, M. L., & Thompson, D. W. J. (2006). Observed relationships between the El Niño–Southern Oscillation and the extratropical zonal-mean circulation. *Journal of Climate*, 19(2), 276–287. <https://doi.org/10.1175/jcli3617.1>
- Liu, J., Curry, J. A., Wang, H., Song, M., & Horton, R. M. (2012). Impact of declining Arctic sea ice on winter snowfall. *Proceedings of the National Academy of Sciences*, 109(11), 4074–4079. <https://doi.org/10.1073/pnas.1114910109>
- Mori, M., Watanabe, M., Shiogama, H., Inoue, J., & Kimoto, M. (2014). Robust Arctic sea-ice influence on the frequent Eurasian cold winters in past decades. *Nature Geoscience*, 7(12), 869–873. <https://doi.org/10.1038/ngeo2277>
- Ogawa, F., Keenlyside, N., Gao, Y., Koenigk, T., Yang, S., Suo, L., et al. (2018). Evaluating impacts of recent Arctic sea ice loss on the Northern Hemisphere winter climate change. *Geophysical Research Letters*, 45(7), 3255–3263. <https://doi.org/10.1002/2017gl076502>
- Outten, S., Li, C., King, M. P., Suo, L., Siew, P. Y. F., Cheung, H., et al. (2023). Reconciling conflicting evidence for the cause of the observed early 21st century Eurasian cooling. *Weather and Climate Dynamics*, 4(1), 95–114. <https://doi.org/10.5194/wcd-4-95-2023>
- Peings, Y. (2019). Ural blocking as a driver of early-winter stratospheric warmings. *Geophysical Research Letters*, 46(10), 5460–5468. <https://doi.org/10.1029/2019gl082097>
- Perlwitz, J., Hoerling, M., & Dole, R. (2015). Arctic tropospheric warming: Causes and linkages to lower latitudes. *Journal of Climate*, 28(6), 2154–2167. <https://doi.org/10.1175/jcli-d-14-00095.1>
- Rantanen, M., Karpechko, A. Y., Lipponen, A., Nordling, K., Hyvärinen, O., Ruosteenoja, K., et al. (2022). The Arctic has warmed nearly four times faster than the globe since 1979. *Communications Earth & Environment*, 3(1), 168. <https://doi.org/10.1038/s43247-022-00498-3>
- Screen, J. A., Deser, C., & Simmonds, I. (2012). Local and remote controls on observed Arctic warming. *Geophysical Research Letters*, 39(10), L10709. <https://doi.org/10.1029/2012gl051598>
- Screen, J. A., Deser, C., Smith, D. M., Zhang, X., Blackport, R., Kushner, P. J., et al. (2018). Consistency and discrepancy in the atmospheric response to Arctic sea-ice loss across climate models. *Nature Geoscience*, 11(3), 155–163. <https://doi.org/10.1038/s41561-018-0059-y>
- Screen, J. A., & Simmonds, I. (2010). The central role of diminishing sea ice in recent Arctic temperature amplification. *Nature*, 464(7293), 1334–1337. <https://doi.org/10.1038/nature09051>
- Sellekvold, R., Sobolowski, S., & Li, C. (2016). Investigating possible Arctic-midlatitude teleconnections in a linear framework. *Journal of Climate*, 29(20), 7329–7343. <https://doi.org/10.1175/jcli-d-15-0902.1>
- Suo, L., Gao, Y., Gastineau, G., Liang, Y.-C., Ghosh, R., Tian, T., et al. (2022). Arctic troposphere warming driven by external radiative forcing and modulated by the Pacific and Atlantic. *Journal of Geophysical Research: Atmospheres*, 127(23), e2022JD036679. <https://doi.org/10.1029/2022jd036679>
- Xu, M., Tian, W., Zhang, J., Screen, J. A., Zhang, C., & Wang, Z. (2023). Important role of stratosphere-troposphere coupling in the Arctic mid-to-upper tropospheric warming in response to sea-ice loss. *npj Climate and Atmospheric Science*, 6(1), 9. <https://doi.org/10.1038/s41612-023-00333-2>
- Xu, X., He, S., Gao, Y., Furevik, T., Wang, H., Li, F., & Ogawa, F. (2019). Strengthened linkage between midlatitudes and Arctic in boreal winter. *Climate Dynamics*, 53(7–8), 3971–3983. <https://doi.org/10.1007/s00382-019-04764-7>
- Xu, X., He, S., Gao, Y., Zhou, B., & Wang, H. (2021). Contributors to linkage between Arctic warming and East Asian winter climate. *Climate Dynamics*, 57(9–10), 2543–2555. <https://doi.org/10.1007/s00382-021-05820-x>
- Xu, X., He, S., Li, F., & Wang, H. (2018). Impact of northern Eurasian snow cover in autumn on the warm Arctic–cold Eurasia pattern during the following January and its linkage to stationary planetary waves. *Climate Dynamics*, 50(5–6), 1993–2006. <https://doi.org/10.1007/s00382-017-3732-8>
- Ye, K., Jung, T., & Semmler, T. (2018). The influences of the Arctic troposphere on the midlatitude climate variability and the recent Eurasian cooling. *Journal of Geophysical Research: Atmospheres*, 123(18), 10162–10184. <https://doi.org/10.1029/2018jd028980>
- Ye, K., & Messori, G. (2020). Two leading modes of wintertime atmospheric circulation drive the recent warm Arctic–cold Eurasia temperature pattern. *Journal of Climate*, 33(13), 5565–5587. <https://doi.org/10.1175/jcli-d-19-0403.1>